# On the evolutions of triple points structure in wedge-stabilized oblique detonations

Zhenye Luan[1], Yue Huang,[1,a] Ralf Deiterding[2], and Yancheng You[1]

AFFILIATIONS

[1] *School of Aerospace Engineering, Xiamen University, Xiamen, 361005, China*

2 *School of Engineering, University of Southampton, Southampton, SO16 7QF, United Kingdom*

[a)] Corresponding author: huangyue@xmu.edu.cn

## ABSTRACT

The oblique detonation induced by a two-dimensional semi-infinite wedge is simulated numerically with the Navier–Stokes equations and a detailed $H_2$/air reaction model based on the open source program-Adaptive Mesh Refinement in Object-oriented C++. A spatially seventh-order-accurate Weighted Essentially Non-Oscillatory scheme is adopted for the convective flux discretization. The formation and evolution of the oblique detonation induced by wedges at different angles and inflow conditions are investigated and a prediction model for oblique detonation flow field is proposed. The results show that the formation of oblique detonation flow field can be divided into two processes. The first process is similar to the oblique shock flow field with unreactive inflow. When the inflow passes through the wedge, the oblique shock wave starts to form at the tip, followed by the unstable curved shock surface and triple point. In this process, a thin reaction layer is formed on the wedge front, but the thickness of the reaction layer is almost constant. The second process is similar to process of deflagration to detonation. As the reaction rate increases, the deflagration front is fixed on the wedge, the reaction layer thickens, and the deflagration front gradually approaches the oblique shock wave. When the deflagration front is coupled with the oblique shock wave, the oblique detonation is formed. Moreover, a theoretical prediction model for the triple point location is proposed. Compared with the numerical simulation results, the theoretical model prediction for the position of the transition point of oblique shock wave-oblique detonation wave is relatively acceptable.

**Keywords:** oblique detonation wave; transition structure; theoretical model prediction; numerical simulation

## 1. INTRODUCTION

An oblique detonation engine (ODE) is a potential propulsion device based on a stationary oblique detonation wave (ODW). The oblique detonation in the combustion chamber is induced by supersonic reactive inflow over a wedge, which is relevant and close to practical configurations for hypersonic propulsion operation. It has received much attention since the 1980s due to its potential advantages of greater efficiency and shorter combustor length in comparison with the traditional scramjet. However, the formation and the stabilization mechanism of an oblique detonation wave (ODW) have not been clearly explained theoretically [1-6].

A wealth of analytic and numerical studies on the fundamental issues about the ODW induced by the wedge can be found in the literatures. The early theoretical solutions of oblique detonations under different shock angles and the ODW structures as the basic foundation were obtained by the pioneering works of Gross [1], Pratt et al. [2], Powers et al. [3,7,8], and Emanuel et al. [9] using reactive Rankine–Hugoniot analysis, in which the ODW is approximated as an oblique shock wave (OSW) coupled with an instantaneous heat release from the reaction zone. The method of characteristics with a one-step Arrhenius chemistry model was developed by Verreault et al. [10] to simulate ODW initiation from a wedge. This resulted in the determination of the wave-angle evolution. A simplified characteristics formulation of linearized Euler equations and linearized Rankine–Hugoniot jump conditions across the leading oblique shock were employed more recently by Martínez-Ruiz et al. [11,12] to analyze the OSW-ODW transition in wedge-induced oblique detonations. The characteristics of wedge-induced OSW-ODW transitions are mainly affected by reaction kinetics. A one-step Arrhenius chemistry model with sufficiently large activation energies can lead to a transition occurring at a triple point for a wide range of combinations of incoming Mach number and wedge angle. Since the detailed flow structure of an oblique detonation under different OSW-ODW transition types is difficult to describe by experimental measurement, high-precision numerical simulation has become the main research method for oblique detonation under high Mach number conditions.

The basic formation structures of an ODW attached to a wedge were first addressed in the pioneering simulation

work of Li et al. [13]; the OSW-ODW transition occurs abruptly at a triple point, which is usually referred to as the abrupt transition mode. The smooth transition mode of the OSW-ODW was first shown in the numerical simulations of Vlasenko et al. [14] and was confirmed in the numerical study by Da Silva et al. [15]. Two distinct OSW-ODW transition modes have been verified numerically for a wide range of chemical kinetics, free-stream Mach numbers, and wedge angles. Ghorbanian and Sterling [16] have numerically analyzed the formation of oblique detonation over a variable-polar-ramp and shown reaction-polar diagrams, suggesting that the formation process of oblique detonation is analogous to DDT. Sislian et al. [17] described the effects of incomplete fuel/air mixing on two types of ramjets performance characteristics by assuming a Gaussian distribution of equivalence ratio in the combustible mixture flow, and the deflagration distortion is observed clearly. The formation and stability of a near-CJ ODW were numerically investigated by Fusina et al. [18]. It was found that the ODW is shown to be resilient to inhomogeneities in the oncoming fuel–air mixture and the induction process and radical formation within the ODW structure were analyzed. Zhang et al. [19] studied the formation of ODW with various equivalence ratio and found that the initiation length as a function of equivalence ratio displays a classical “V-shaped” curve, similar to the relation between detonation cell size and initiation energy [20]. Iwata et al. [21] simulated the shock-induced combustion from a supersonic spherical projectile, illustrating several shock-flame configurations induced by inflow equivalence ratio inhomogeneity. They also performed simulations on wedge-stabilized oblique detonations [22] with different Gaussian equivalence ratio distributions, demonstrating that the near-wedge deflagration fronts are distorted into a complicated surface, generating the so-called “V-shaped” deflagration front and “V+Y” Mach stem. Fang et al. [23] focused on the formation and characteristic parameters of the oblique detonation wave with inhomogeneous mixing of hydrogen and air inflow for a better understanding of oblique detonation wave engine performance under practical operating conditions. Bachman and Goodwin [24] presented a new ignition criterion curve that was added to the traditional stability limits in order to include the effects of chemical kinetic timescales and wedge surface length on the prediction of ignition and formation of ODWs. This ignition criterion was demonstrated to accurately predict

formation and ignition location of an ODW on an inviscid wedge surface. Since two-dimensional numerical simulations are computationally demanding, numerical studies tend to focus on a limited number of cases (e.g., by fixing the wedge angle or the incoming stream's properties), so that only limited portions of the accessible parametric space are explored. As a result, despite significant work, there is still a lack of a complete parameter specification for ODW formation, which makes it impossible to predict the structure and the transition type of ODW.

This paper analyzes the change of the relative position of flame and OSW in the process of the establishment of ODW flow field. The influence of different wedge angles on the flow field in the engine in real situation is simulated in the hope of summarizing some rules for the prediction of oblique detonation structure. The paper is organized as follows. Section 2 summarizes the numerical methods used to solve the equations and the calculation model for the simulations. In Section 3, the AMROC code and the convergence of grid resolution is verified. Section 4 analyses the results and discuss the formation of ODW flow field and the gradual combustion enhancement process during the formation of ODW. Section 5 contains our conclusions.

## 2. NUMERICAL METHOD AND CALCULATION MODEL

### 2.1. Numerical method

The system of governing equations are the two-dimensional compressible reactive Navier–Stokes equations, which we write in the form of an inhomogeneous convection-diffusion equation as

$$\frac{\partial Q}{\partial t}+\frac{\partial\left(F_x-G_x\right)}{\partial x}+\frac{\partial\left(F_y-G_y\right)}{\partial y}=S\,, \tag{1}$$

In Equation (1), $Q$ is the vector of state quantities, $F_x$ and $F_y$ are the convective fluxes, and $S$ is the chemical reaction source term, which are defined as

$$Q=\begin{bmatrix}\rho_i\\ \rho u\\ \rho v\\ \rho E\end{bmatrix},\quad F_x=\begin{bmatrix}\rho_i u\\ \rho u^2+p\\ \rho uv\\ u\left(\rho E+p\right)\end{bmatrix},\quad F_y=\begin{bmatrix}\rho_i v\\ \rho uv\\ \rho v^2+p\\ v\left(\rho E+p\right)\end{bmatrix},\quad S=\begin{bmatrix}\dot{\omega}_i\\ 0\\ 0\\ 0\end{bmatrix}, \tag{2}$$

where $i$=1,2...$N_{sp}$ and $N_{sp}$ is the number of species. In Equation (1), $G_x$ and $G_y$ are the fluxes of the diffusion terms,

which are defined as

$$G_x = \begin{bmatrix} \rho D_i(\partial Y_i / \partial x) \\ \tau_{xx} \\ \tau_{xy} \\ k(\partial T / \partial x) + \rho \sum_{j=1}^{N_{sp}} h_j D_j (\partial Y_j / \partial x) + u\tau_{xx} + v\tau_{xy} \end{bmatrix}, \tag{3}$$

$$G_y = \begin{bmatrix} \rho D_i(\partial Y_i / \partial y) \\ \tau_{yx} \\ \tau_{yy} \\ k(\partial T / \partial y) + \rho \sum_{j=1}^{N_{sp}} h_j D_j (\partial Y_j / \partial y) + u\tau_{xy} + v\tau_{yy} \end{bmatrix}. \tag{4}$$

In Equations (3) and (4), $Y_i$ is the mass fraction of component *i* in the mixed gas, $D_i$ and $D_j$ represent the mixture diffusion coefficients, $k(\partial T / \partial x)$ and $k(\partial T / \partial y)$ represent the energy fluxes caused by heat conduction, $\rho \sum_{j=1}^{N_{sp}} h_j D_j (\partial Y_j / \partial x)$ and $\rho \sum_{j=1}^{N_{sp}} h_j D_j (\partial Y_j / \partial y)$ represent the energy fluxes caused by species diffusion, and $\tau$ is the viscous stress tensor, which is specified as

$$\tau_{xx} = -(2/3)\mu(\nabla \cdot \mathbf{v}) + 2\mu(\partial u / \partial x), \quad \tau_{yy} = -(2/3)\mu(\nabla \cdot \mathbf{v}) + 2\mu(\partial v / \partial y), \tag{5}$$

$$\tau_{xy} = \tau_{xy} = \mu(\partial u / \partial y + \partial v / \partial x), \text{ with } \nabla \cdot \mathbf{v} = (\partial u / \partial x + \partial v / \partial y). \tag{6}$$

In addition, *E* in Equation (1) is the total energy per unit mass, which reads

$$E = \sum_{i=1}^{N_{sp}} Y_i h_i - p / \rho + \frac{1}{2}(u^2 + v^2). \tag{7}$$

The quantity $h_i$ is the specific enthalpy of component *i*, which reads for a thermally perfect gas

$$h_i = h_{\text{ref}}^0 + \int_{T_{\text{ref}}}^{T} c_{p_i} dT. \tag{8}$$

The variable $\dot{\omega}_i$ is the mass generation rate of component *i*, which can be obtained by a detailed chemical reaction mechanism consisting of *J* reactions as

$$\dot{\omega}_i = \sum_{j=1}^{J} (\nu_{ji}^r - \nu_{ji}^f) \left[ k_j^f \prod_{n=1}^{N_{sp}} (\rho_n / W_n)^{\nu_{jn}^f} - k_j^r \prod_{n=1}^{N_{sp}} (\rho_n / W_n)^{\nu_{jn}^r} \right], \ i = 1, \ldots N_{sp}, \tag{9}$$

where $\nu_{ji}^{f}$ and $\nu_{ji}^{r}$ represent stoichiometric coefficients of forward and reverse chemical reaction. $W_n$ represents the molar mass of component *i*. The forward and reverse chemical reaction rate constants are given by Arrhenius formulas:

$$k_j^{f/r}(T) = A_j^{f/r} T^{\beta_j^{f/r}} \exp\left(-E_j^{f/r} / RT\right). \quad (10)$$

In Equation (10), activation energy and pre-exponential factor refer to the corresponding chemical reaction mechanism. The ideal gas equation for mixtures is used to close the system of Equation (1).

The numerical simulations have been carried out using the open-source code AMROC [25,26] based on a structured adaptive mesh refinement (SAMR) framework [27]. An operator splitting technique (or, the method of fractional steps) for the computation of the time-dependent reactive flow (see [28]) is used to solve Equation (1). This technique allows a decoupled treatment for the time-implicit discretization of the local source term and the time-explicit discretization of the hydrodynamic transport term. The convection terms in Equation (1) are discretized with the seventh-order WENO-symmetric-order optimized (WENO-SYMOO) scheme as shown by Martin et al. [29]. The optimal third-order strong stability preserving (SSP) Runge-Kutta scheme [30] is used for time integration in combination with time-splitting and the fourth-order accurate semi-implicit GRK4A method [31] for source term integration. A detailed $H_2$-Air reaction mechanism including 9 species ($O_2$, $H_2O$, H, O, OH, $H_2$, $HO_2$, $H_2O_2$, $N_2$) and 34 elementary reactions has been used [32].

## 2.2. Calculation model

Fig. 1 shows the two-dimensional computational domain and boundary conditions. The two-dimensional rectangular region is selected to make the boundary and structured grid parallel to the Cartesian coordinate axis (*X*-axis and *Y*-axis), respectively, so as to eliminate the calculation error caused by the otherwise non-Cartesian oblique boundary. The left boundary and upper boundary are free stream boundary conditions. The right boundary is opened to the atmosphere with the outflow boundary condition. The lower boundary represents the wedge surface that is set as no-slip boundary condition. The angle between the free stream and the *X*-axis is $\theta$.

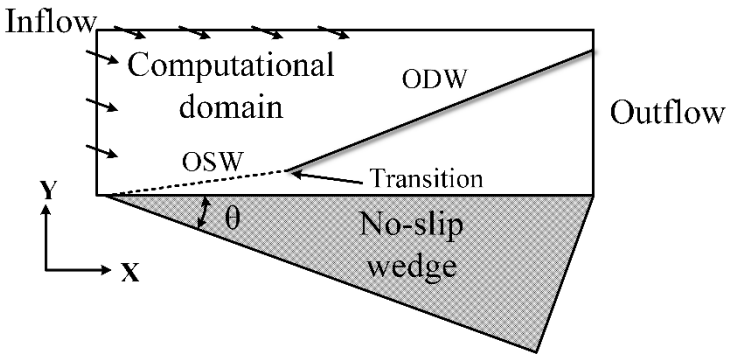


**Fig. 1** Schematic of the computational domain and boundary conditions

The free stream is a mixture of hydrogen, oxygen and nitrogen with a mole fraction ratio of 2: 1: 3.76. The difference of oblique detonation flow field is compared when the wedge angle $\theta$ is 15° (case1), 20° (case2) and 25° (case3). Considering a flight altitude of 30 km and a flight Mach number of 10, the ambient flow is pre-compressed twice by weak oblique shock waves in the aircraft inlet. The deflection angle is 12.5°. Therefore, the inflow temperature of 1021K, the inflow pressure of 56kPa, and inflow Mach number of 4.3 are obtained [33]. The computational domain along the *X*- and *Y*- axis are (−1mm, 79mm), (0, 20mm), respectively. The position of the vertex of the wedge in the computational domain is (0mm, 0mm). The computational base cell size is set to 25μm × 25μm and refined to up to 3.125μm × 3.125μm adaptively on-the-fly. The half reaction length (hrl) is 0.59314mm for the current initial conditions, as calculated by Cantera [34], which corresponds to about 190 points per half reaction length (190 pts/ hrl).

## 3 VERIFICATION OF CODE AND GRID RESOLUTION

To verify the accuracy of the numerical simulation, the model and grid resolution are validated. First of all, based on the work by Viguier [35], the comparison of numerical and experimental ODW field with the results calculated by the code in this paper are displayed in Fig. 2 with the same inflow conditions. As can be seen in Fig. 2a, the numerical schlieren of ODW field calculated by AMROC agree well with the experimental ODW field. Typical structures and phenomena can be clearly distinguished: OSW, triple point ODW slip line and transverse wave. Similarly, the comparison of numerical simulation results is also highly consistent, as shown in Fig. 2b. Moreover,

the method of characteristics (MoC) is an exact method for steady supersonic flow when the number of characteristics is sufficient. In the previous paper [36], the numerical methods of AMROC are compared with those using the method of characteristics (MoC) [10]. The AMROC solutions are in excellent agreement with the MoC results. Therefore, the above proves the reliability of the code (AMROC) used in this paper.

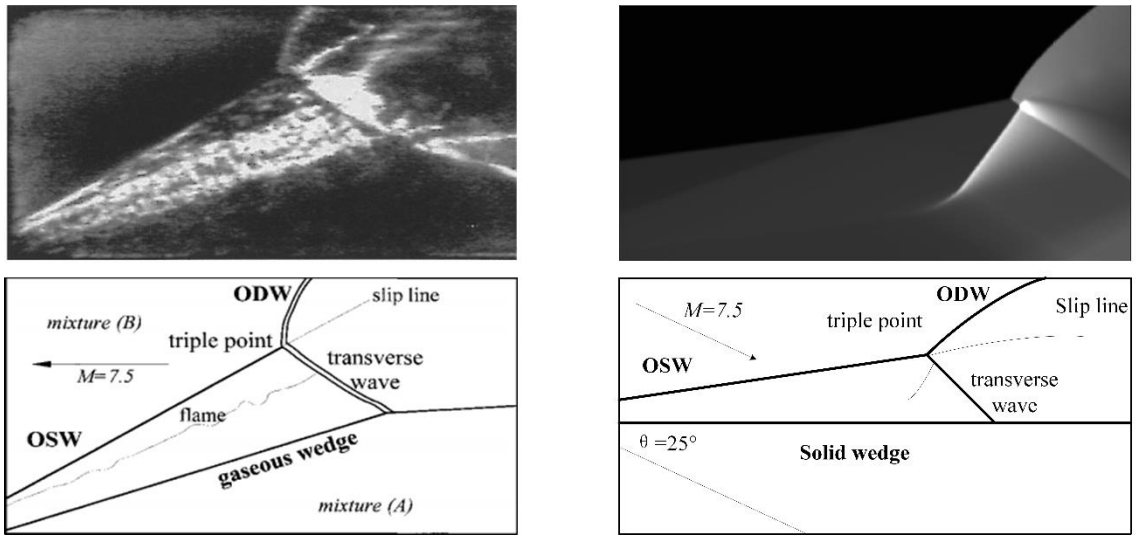


**(a) Comparison of experimental schlieren from Viguier [35] (left) and numerical schlieren using AMROC (right)**

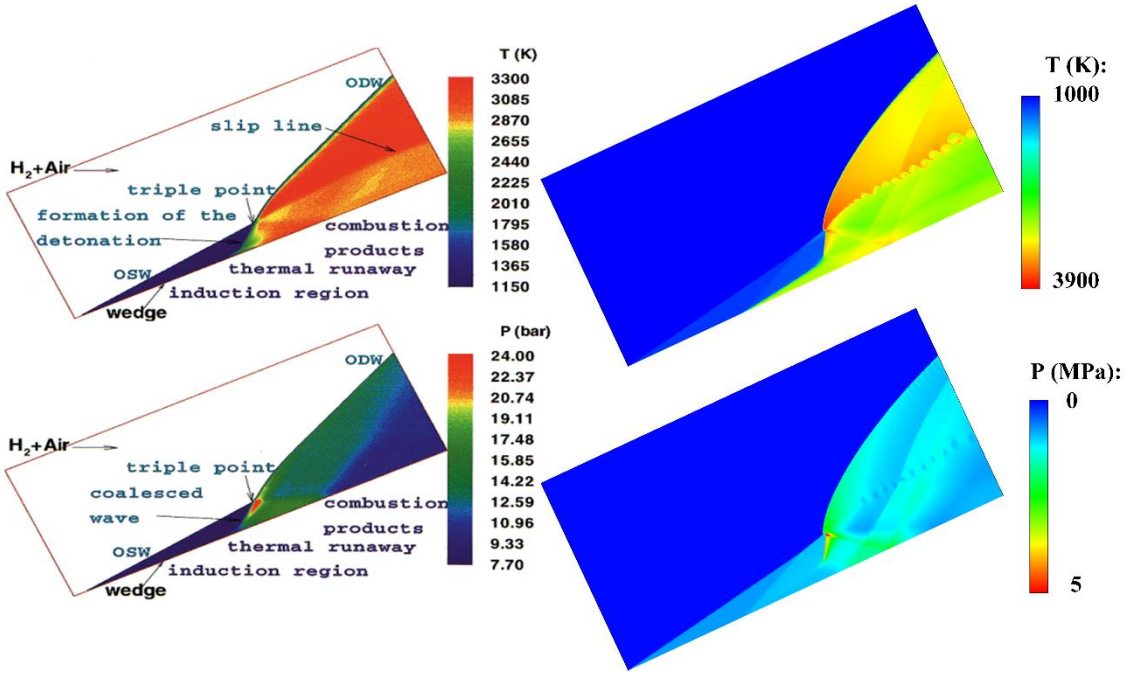


**(b) Comparison of numerical results between Viguier [35] (left) and simulation using AMROC (right)**

**Fig. 2 Comparison of numerical and experimental results between Viguier [35] and simulation using AMROC**

The numerical detonation simulation results are sensitive to the grid length scale. Two scales of mesh are

selected for a mesh resolution and convergence study to ensure the independence of the results with respect to the grid scale. Coarse mesh: minimum mesh size is 6.25μm × 6.25μm for level 3 refinement; Fine mesh: minimum mesh size is 3.125μm × 3.125μm for level 4 refinement. And the refinement factor is set as 2 for each level. As shown in Fig. 3, the structures of the oblique detonation wave system obtained are basically consistent and difficult to distinguish. A quantitative comparison is conducted by plotting the pressure and temperature along three typical lines (i.e. y = 0 mm, 2 mm and 10 mm), as shown in Fig. 4. These lines correspond to different flow regions of the ODW field, including the wedge surface, OSW surface and steady ODW surface. The curves nearly overlap with trivial differences. Therefore, coarse mesh (6.25μm × 6.25μm for level 3 refinement) is sufficient to capture the main ODW structures. To capture the structure of ODW flow fields in more detail, the fine mesh (3.125μm × 3.125μm for level 4 refinement) is selected in this paper.

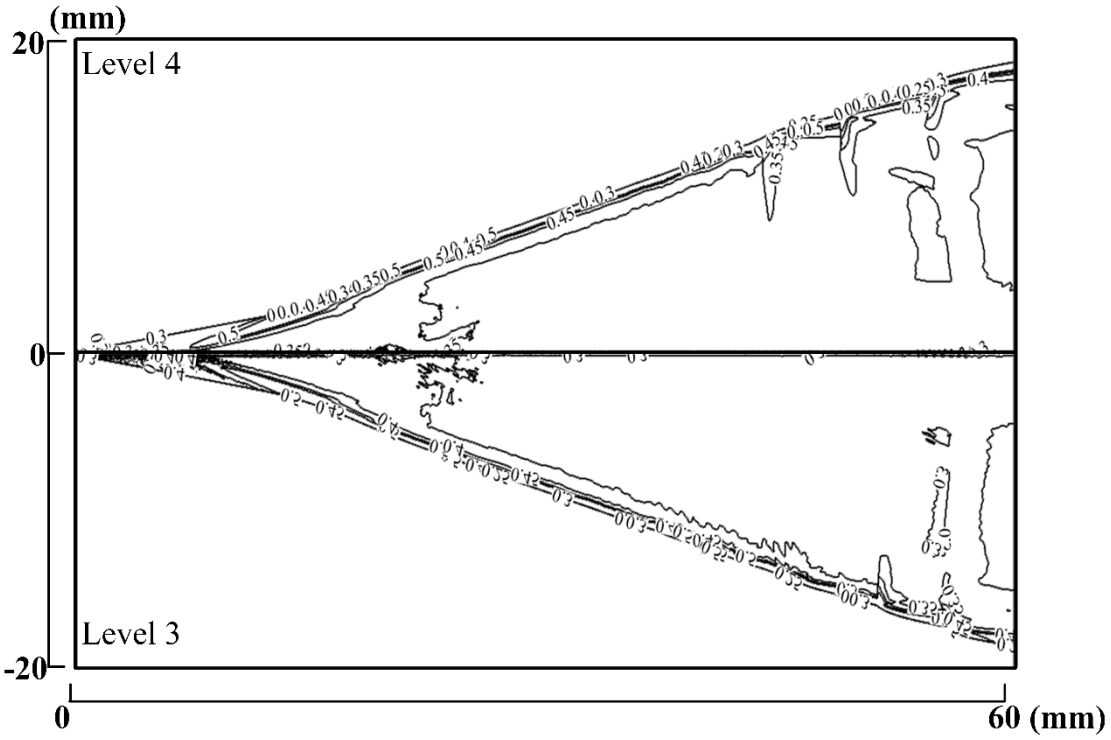


**Fig. 3 Density fields with different grid scales in the case2**

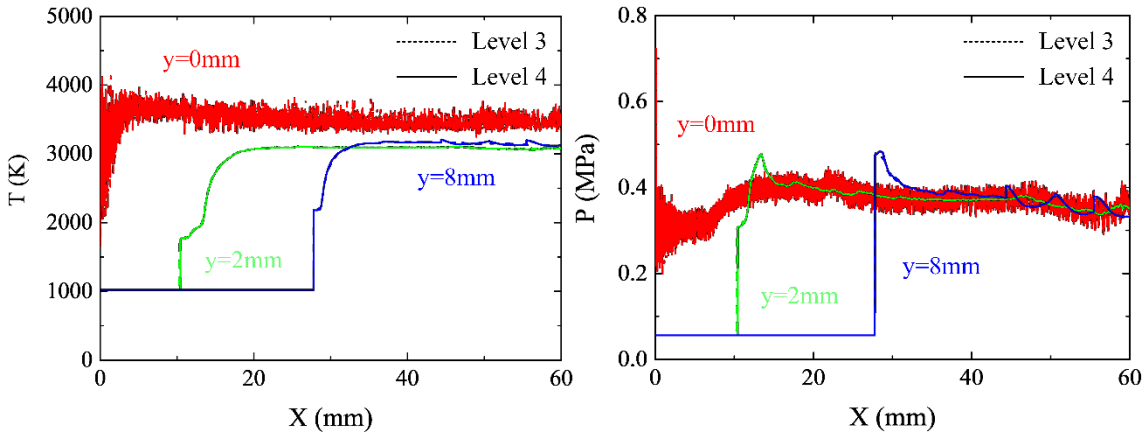


**(a) Temperature** **(b) pressure**

**Fig. 4 (a) Temperature and (b) pressure along different lines parallel to the *X*-axis with different grid scales in the case2**

## 4. RESULTS AND DISCUSSION

### 4.1. The formation of smooth oblique detonation

Fig. 5 shows the diagram of Mach number and locally enlarged temperature and pressure at t=2.5μs when the ODW flow field is established, as well as the parameters variation curve along the streamline of case2. Based on the changes of temperature, pressure and components on the streamline, first of all, an OSW is generated at the tip of wedge when inflow enters the flow field. The flow field downstream is not stable, so a weak compression wave (CW) is formed between the OSW and the flow field downstream to balance the pressure in the flow field. A triple point is formed on the shock front and moves downstream. A thin chemical reaction layer is formed on the wedge surface, which shows KH instability near the wedge surface as well as slip line. However, the chemical reaction is slow at this time, the flow field is similar to that of unreactive flow.

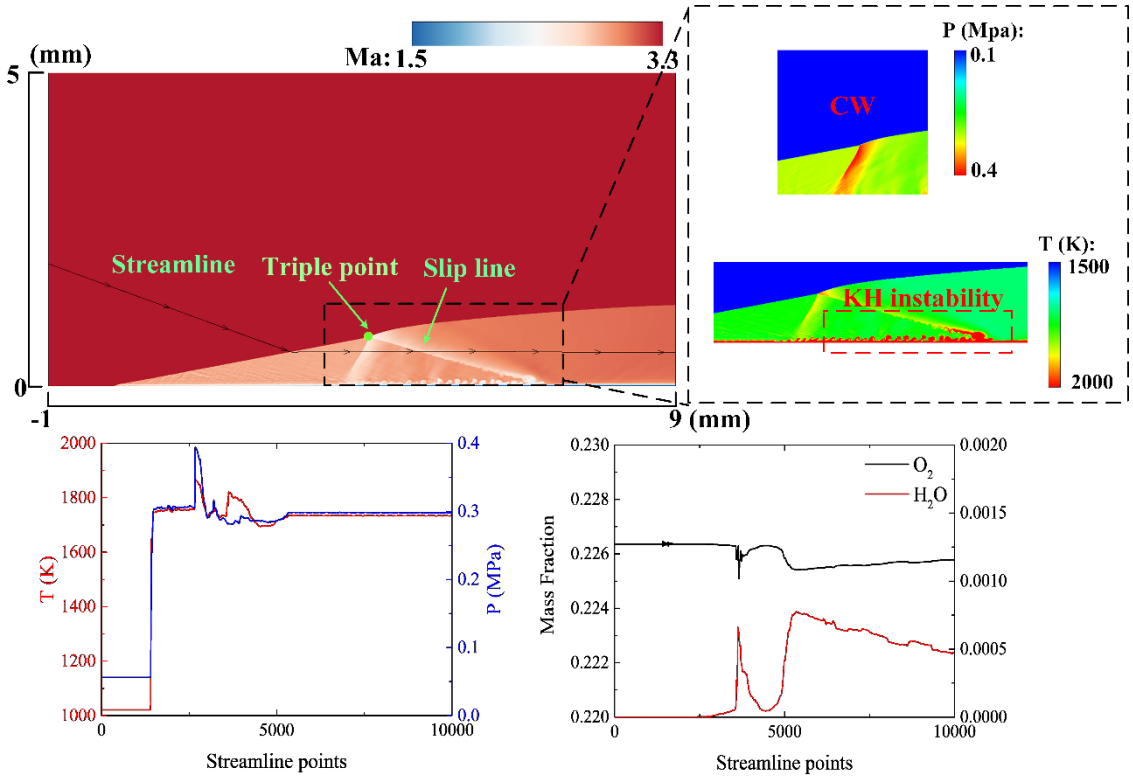





**Fig. 5 Diagram of Mach number, local enlarged temperature and pressure at t=2.5μs, and the parameters variation curve along the streamline of case2**

With the passage of time, the diagram of Mach number, local enlarged pressure, and parameters variation curve along the streamline in the flow field of case2 at t=14.8μs are shown in Fig. 6. The expansion rate of the reaction front becomes faster, the reaction layer becomes thick, the chemical reaction rate accelerate, and the deflagration surface begins to form. With the expansion of the combustion products, the distance between the deflagration surface and the OSW (induction length) decreases, and the intensity of deflagration gets higher, approaching CJ conditions. Moreover, the new triple points are formed and propagate downstream along the wave front, which stabilizes the front of OSW and ODW behind. It indicates that the motion of the triple points can stabilize the uneven internal flow field until a stable ODW is formed.

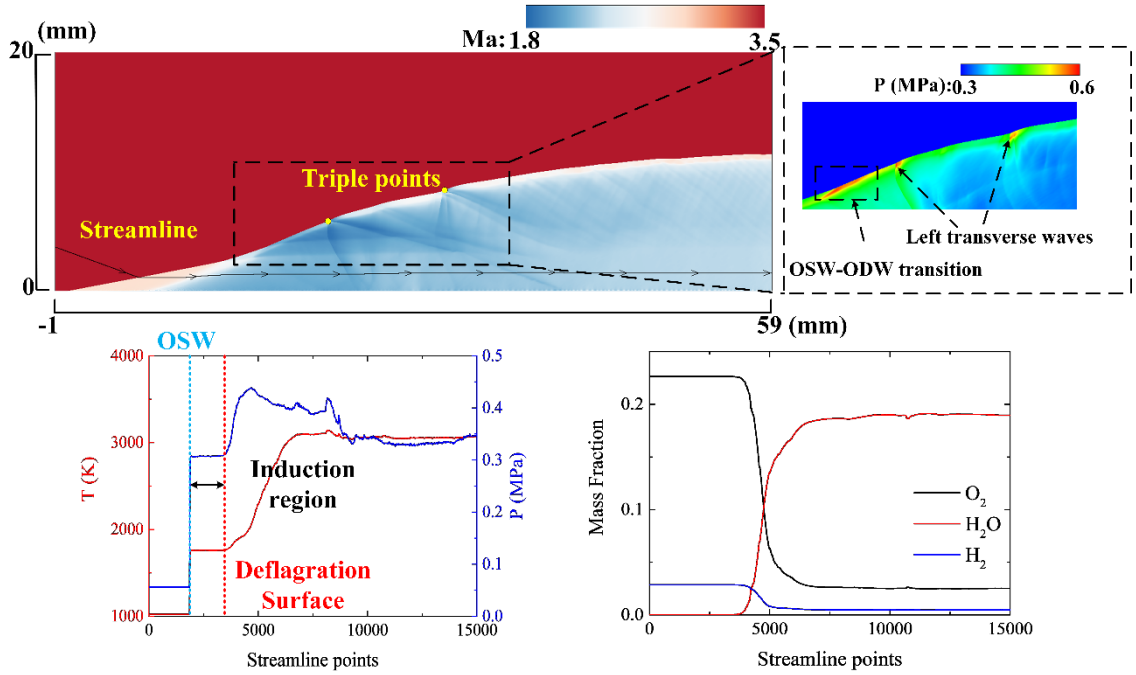


198

199 **Fig. 6 Diagram of Mach number, local enlarged pressure at t=14.8μs, and the parameters variation curve along the streamline**

200 **of case2**

201 Figure 7 shows the pressure in the flow field and the motion of triple points at different times after OSW-ODW

202 transition of case2. Before the formation of the first triple point, the front of ODW is highly unstable, indicating that

203 the pressure fluctuation frequency is high, but the amplitude is not large. After the formation of the triple points, the

204 pressure fluctuation between the triple points decreases in frequency but increases in amplitude. This is manifested

205 by the lengthened distance between transverse waves and the increased peak pressure of triple points. Finally, the

206 ODW surface becomes smooth, and the parameters before and after the ODW are stable.

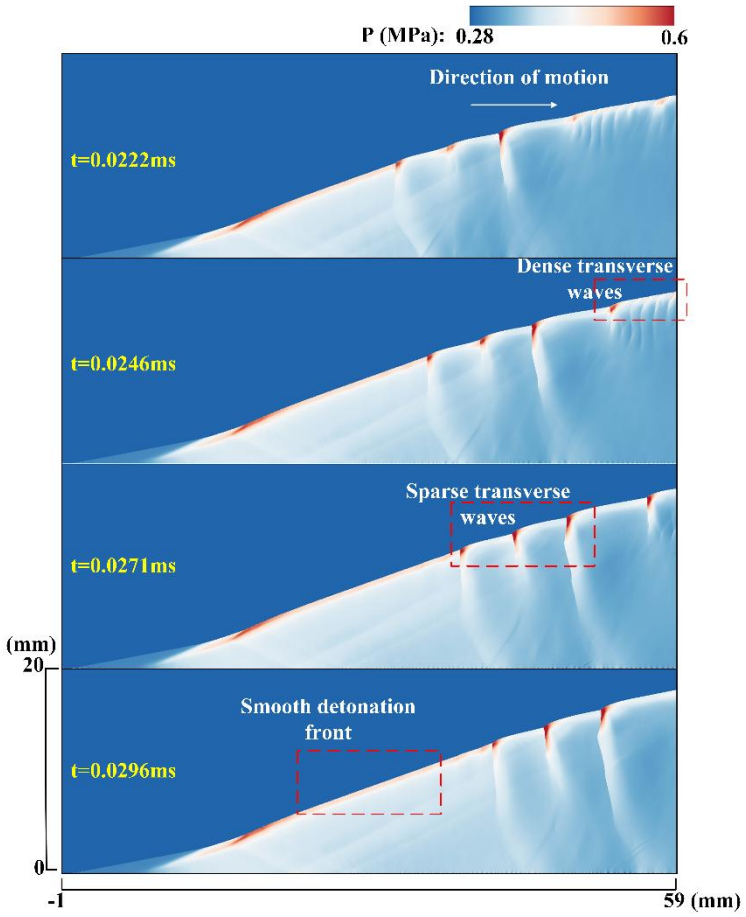


**Fig. 7 Diagram of pressure in the flow field after OSW-ODW transition at different times of case2**

The parameters of a line parallel to the *Y*-axis and crossing the stable ODW front (e.g. *x*=30 in Fig.7) are extracted, as shown in Fig. 8.The dashed line represents the CJ temperature and pressure calculated by Cantera [34] under the conditions of inflow in this paper, which are 3012K and 2.5bar respectively. The induction length is 0.36mm. Compared with the CJ value, the temperature in the flow field is similar, the pressure is slightly higher, and the induction length is slightly lower, which is 0.28mm. In general, the numerical simulation results are close to the ZND solution, which proves the reliability of the numerical simulation results in this paper again.

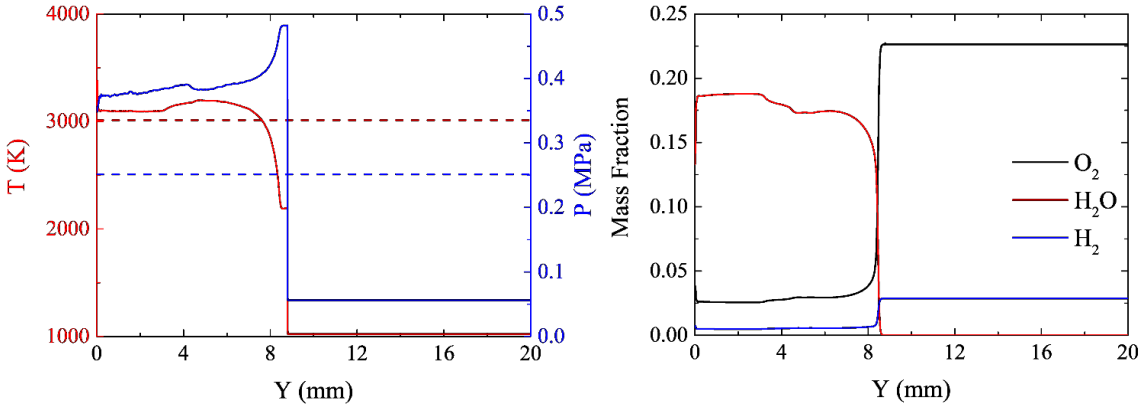


**Fig. 8 Temperature, pressure, components along x=30mm in Fig. 7**

Fig. 8 shows the smooth transition structure and a more detailed triple point structure. The main structure of transition is two compression waves accompanied by chemical reaction, and the front of waves is unstable. A more detailed schematic structure is shown in Fig. 11. Similarly, the detailed structure of the triple points is also enlarged. It can be found that there is a Mach stem between the transverse wave, OSW and ODW, and a shock wave is used to balance the pressure of the flow field near the triple points, therefore the final structure of triple point is y-shaped.

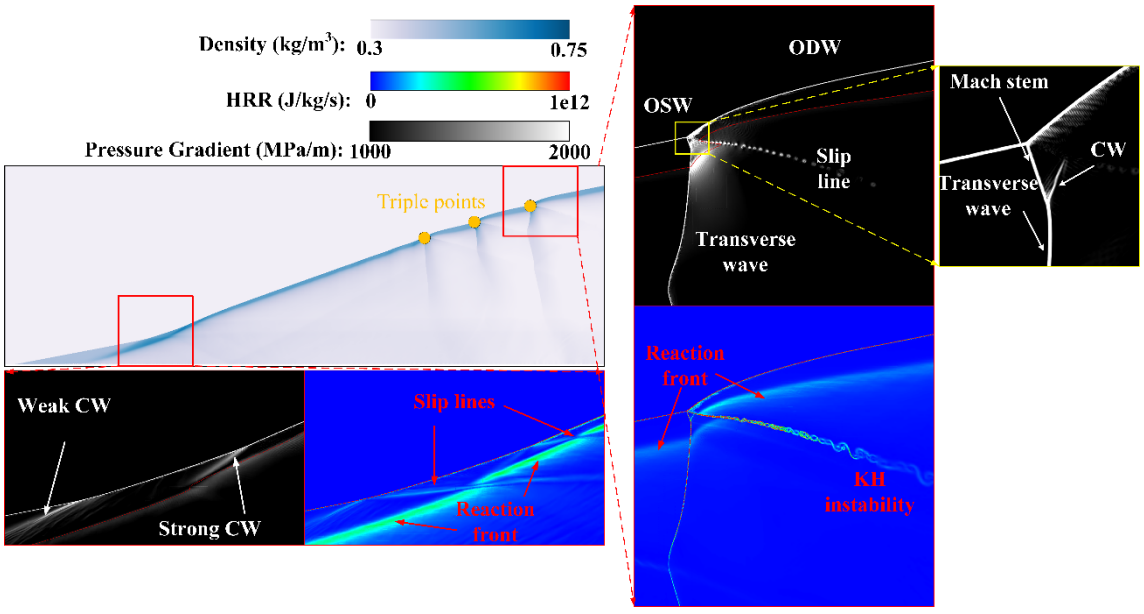


**Fig. 9 Enlarged diagram of smooth transition structure and triple points structure**

Pressure traces along different streamline lines through the transition structure of the flow field in Fig. 9 are shown in Fig. 10. The compression strength of the fluid passing through OSW on streamline 1 is the same as that on streamline 2, but the burning strength of the deflagration surface on streamline 1 is lower than that on streamline 2.

Pressure peaks on streamlines 3 and 4 are almost the same and higher than streamlines 1 and 2, indicating that the OSW on streamlines 3 and 4 has been transformed into an ODW. The differences are that the detonation front on streamline 4 is an overdriven detonation, and the inflow pressure is compressed to a value higher than stable ODW, as compared with Fig. 8. The first compression of inflow on streamline 3 is almost the same as that of stable ODW, but after that, the inflow does not expand and decompress, but continues to be compressed until it reaches the intensity of overdriven detonation wave, which is called transitional detonation in this paper.

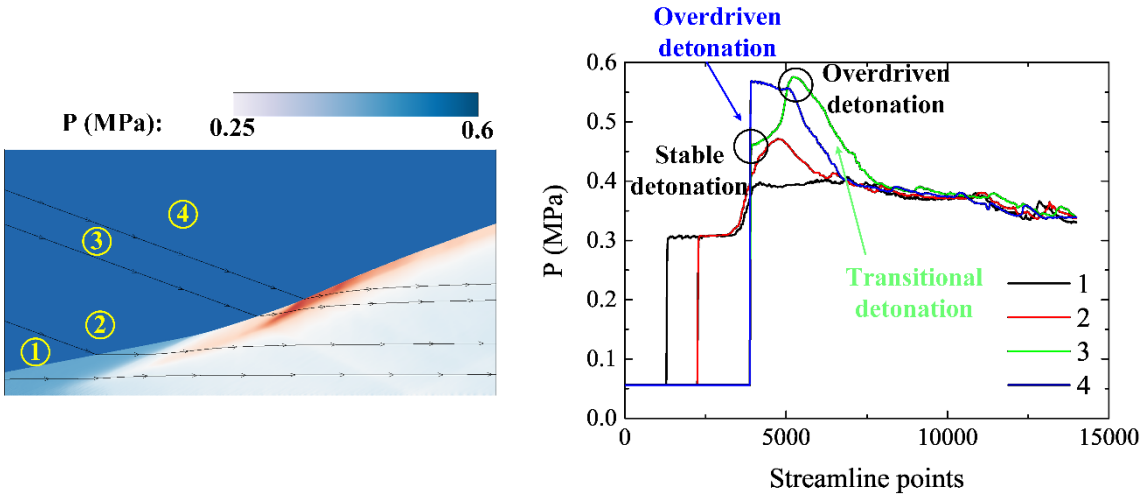


**Fig. 10 Pressure on different streamline lines through smooth transition structure of the flow field in Fig. 9**

Based on the analysis above, the detailed schematic structure at the smooth transition position of OSW-ODW is extracted, as shown in Fig. 11. There is a curved transitional detonation wave between the OSW and ODW, and the three waves are separated by two compression shock waves. The temperature and density of the flow field after the three waves are discontinuous, while the velocity and pressure are continuous, resulting in two slip lines. The two transitional compression shock waves and the reaction front generate reflected shock waves at the slip line. The position with higher heat release rate (HRR) represents the position of the reaction front, and a discontinuity occurs at the position of the slip lines. When the OSW-ODW transition occurs, the pressure is the highest, and the overdriven detonation is generated and then decays to a CJ detonation.

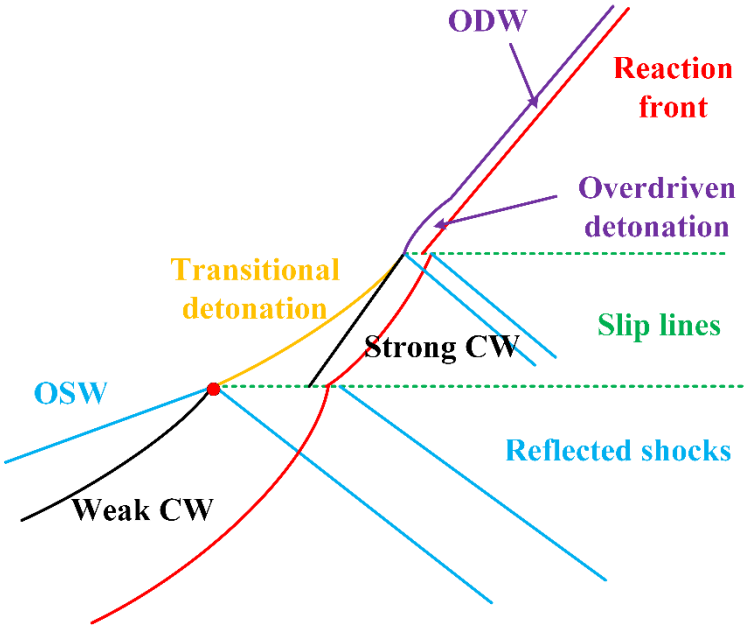


**Fig. 11 Schematic of detailed structure at the smooth transition position of OSW-DOW**

The variation of parameters and structures in the process of the establishment of the ODW flow field is analyzed in this section. More importantly, the detailed triple points structure and schematic diagram of OSW-ODW transition structure is extracted. Similar to the DDT process, the transition process and structure are analyzed in detail, which provides a certain reference for the prediction of ODW flow field structure.

### 4.2. The formation of abrupt oblique detonation

The formation of ODW and the smooth transition structure of OSW-ODW is analyzed in detail in Section 4.1. In this section, the inflow temperature, pressure and Mach number in case2 were changed to 765K, 33.5kPa and 3.94, respectively, to form an abrupt-type ODW and analyze its transition structure. Firstly, the initial OSW flow field and the reaction layer thickening process are the same as the smooth-type ODW in Section 4.1. However, due to the decrease of inflow energy, the OSW-ODW structure changes, as shown in Fig. 12. In contrast to smooth-type ODW, the relative position of the transitional detonation, overdriven detonation and the triple point are changed.

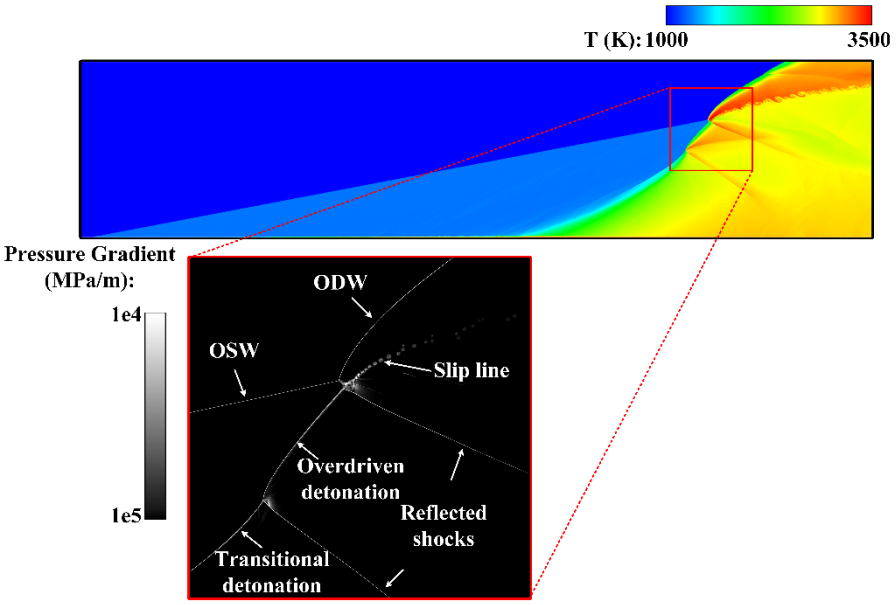


**Fig. 12 Enlarged diagram of abrupt transition structure**

Similar to Fig. 10, streamlines at four typical positions in the OSW-ODW transition structure were taken and the pressure on the streamlines was compared, as shown in Fig. 13. The pressure variation on the four streamlines is the same as that on the streamlines of smooth-type ODW in Fig. 10. The only difference is that in the smooth-type ODW, the triple point is formed by OSW, transitional detonation and weak CW. However, now the triple point is formed by OSW, ODW and overdriven detonation in the abrupt-type ODW, as shown in Fig. 14. The angle and intensity of OSW change when the inflow Mach number is reduced. The energy of inflow is lower after being compressed by OSW, so the induction time is longer, resulting in an increase in the formation time of ODW. In this process, the upward expansion velocity of combustion products is so fast that it affects the flow parallel to the wedge, which can be seen from the deflection angle of the streamline lines. And the deflagration surface quickly approaches the weak CW behind the OSW and transitional detonation and overdriven detonation are generated. Finally, the position of the triple point is stable on the ODW, forming the shape of abrupt-type ODW. In this process, because the intensity of the OSW and ODW differs greatly and there is no transition wave between OSW-ODW, , resulting in the formation of Mach stem at the triple point to form a y-shaped structure, similar to the triple points downstream of the smooth-type ODW in Fig. 9.

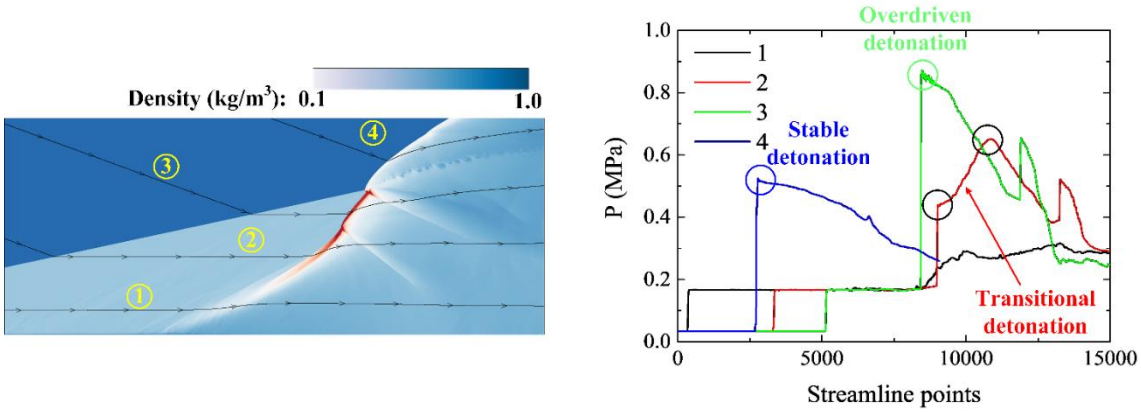


272

273 **Fig. 13 Pressure on different streamline lines through abrupt transition structure**

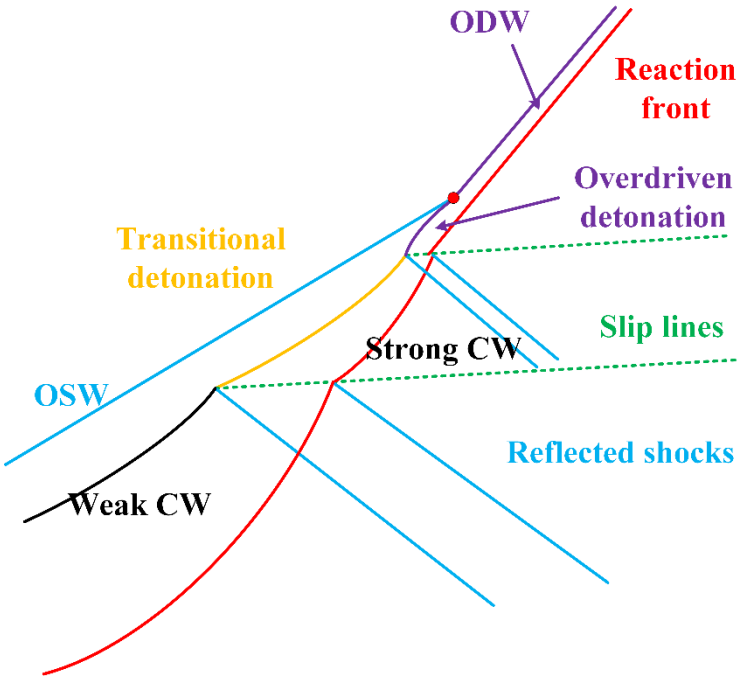


274

275 **Fig. 14 Schematic of detailed structure at the abrupt transition position of OSW-DOW**

276 4.3. A method of transition point prediction for oblique detonations

277 In the process of the establishment of the ODW flow field, the OSW compresses the pressure and temperature
278 of the reactants, and then the rapid chemical reaction begins at some point near the wall. In the process of rapid
279 expansion of combustion products, the angle between the deflagration surface and the wall is greater than that
280 between the OSW and the wall. In the direction normal to the OSW, the deflagration flame gradually approaches the
281 OSW, and then the ODW is generated. Based on Sections 4.1 and 4.2, a theoretical model for predicting the position
282 of the triple point is proposed in this section, which is of certain reference for predicting the structure of oblique

detonation flow field. The following is a detailed analysis of this process.

Fig. 15 is a schematic diagram of the ODW flow field. Firstly, the turning angle of the first OSW can be obtained by Eq. 11 in gas dynamics,

$$\frac{\tan(\beta_1+\theta)}{\tan\beta_1}=\frac{(\gamma+1)M_1^2\sin^2(\beta_1+\theta)}{(\gamma-1)M_1^2\sin^2(\beta_1+\theta)+2}. \tag{11}$$

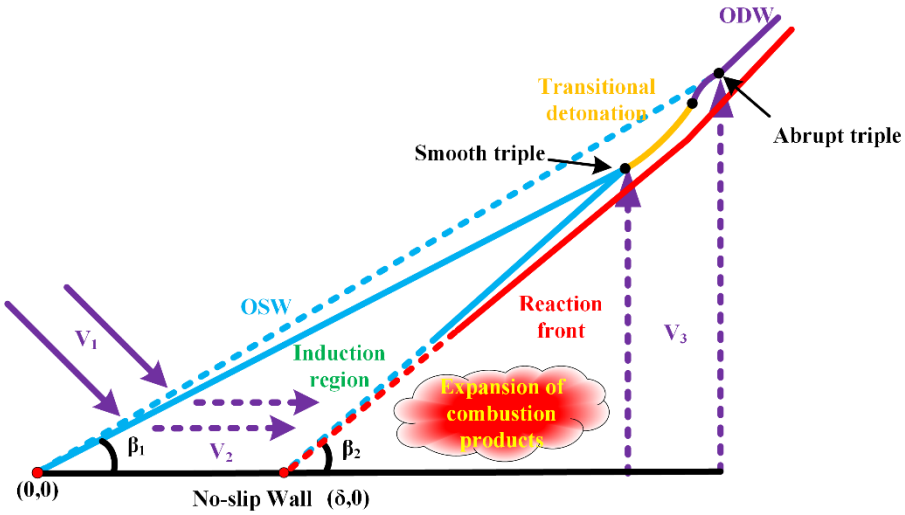


**Fig.15 Schematic diagram of ODW flow field**

In the ODW flow field, the angle of OSW and the inflow Mach number basically satisfy Eq. 11, indicating that the first OSW has nothing to do with whether the inflow is reactant. Thus, $\beta_1$ is determined when the inflow Mach number is constant. Based on Fig. 11,

$$\tan\beta_1=\frac{y}{x}=\frac{V_3t}{\delta+V_2t},\ \tan\beta_2=\frac{y}{x-\delta}=\frac{V_3t}{V_2t}. \tag{12}$$

Due to the slow combustion rate of deflagration surface, the parameters such as pressure, temperature and velocity change slowly. $V_2$ is considered as a constant value, which can be directly calculated by Eq. 11. The γ before and after OSW and ODW is assumed to be a constant, respectively. $V_3$ is the expansion velocity of combustion products, that is, the deflagration velocity. As the reaction layer thickens from the wedge, the flame surface remains flat. It can be considered that the maximum deflagration velocity is reached when the products begin to expand. According to CJ theory, the maximum deflagration velocity is about 1/2 of CJ detonation velocity. Under the assumption above, the position of the triple point and the angle of the deflagration surface can be simply predicted.

Based on the above prediction model, the pressure gradient diagrams of case1, case2, case3 and abrupt case are shown in Fig. 16. The yellow dots represent the position of the triple point. The red line represents half of the $H_2O$ mass fraction after complete reaction in the flow field, and the position of the rapid reaction, which is defined as the deflagration surface or reaction front in this paper. Fig. 16 proves the theoretical analysis of the interaction of the deflagration surface and ODW and structure changes in the formation process of ODW in section 4.1 and 4.2.

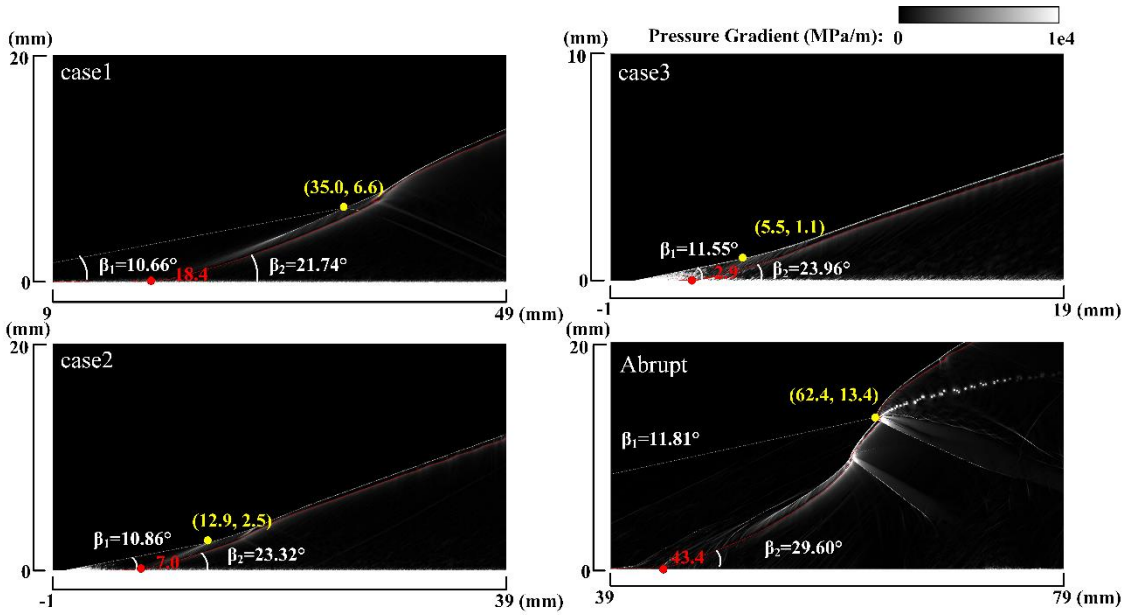


**Fig. 16 Verification of the prediction model of ODW flow field**

Table 1 summarizes the relevant parameters required by the prediction model above and the comparison between the prediction and the simulation results at different cases, in which the parameters with upper quotes is the theoretical predicted values, otherwise is the numerical simulation values . After passing the first OSW, the movement direction of inflow is parallel to the wall, and the reaction layer becomes thick at a certain point that is defined as the deflagration surface starting point δ. It can be found from the table that the δ and angle of the deflagration surface $\beta_2$ are greatly affected by the wedge angles. The larger the wedge angle, the faster the reactants combust, the closer the δ is to the vertex of the wedge, and the larger the angle of the deflagration surface is. The theoretical prediction error of the triple point position is about a few millimeters, which is small enough to be acceptable. It is worth mentioning that in the whole prediction model, all parameters are derived theoretically, and only δ is extracted from the simulation

results. This means that as long as the determination method of δ is given, the basic configuration of ODW flow field can be roughly described theoretically under given flow conditions. Therefore, future work will focus on the derivation of δ and the improvement of the model.

**Table 1. Comparison of parameters of theoretical prediction model in different ODW flow fields**

| | θ (°) | δ (mm) | $M_2$ | $V_2$ (m/s) | $\beta_1$ (°) | $\beta_2$ (°) | $\beta_2$' (°) | (x, y) (mm, mm) | (x', y') (mm, mm) |
|---|---|---|---|---|---|---|---|---|---|
| **case1** | 15 | 18.4 | 3.22 | 2983 | 10.66 | 21.74 | 17.40 | (35.0, 6.6) | (46.0, 8.7) |
| **case2** | 20 | 7.0 | 2.85 | 2865 | 10.86 | 23.32 | 18.07 | (12.9, 2.5) | (17.0, 3.3) |
| **case3** | 25 | 2.9 | 2.47 | 2701 | 11.55 | 23.96 | 19.09 | (5.5, 1.1) | (7.1, 1.4) |
| **abrupt** | 20 | 43.4 | 2.54 | 1942 | 11.81 | 29.60 | 25.92 | (62.4, 13.4) | (76.2, 15.9) |

This section proposes a simple theoretical prediction model that predicts the triple point. The prediction model is analyzed and verified in detail and compared with the flow field obtained by numerical simulation. The results show that, based on the assumptions in this paper, the error of the theoretical prediction model for the position of the triple point is relatively acceptable for such a simplified model. However, in order to predict the flow field of ODW more accurately, improvement is necessary, which is also the main work in the future.

## 5. CONCLUSIONS

In this study, two-dimensional simulations are carried out in order to investigate the formation and evolution of the oblique detonation induced by wedges at different angles and inflow conditions, a detailed model of transition structure of OSW-ODW is analyzed and a theoretical prediction model that predicts the triple point is proposed.

The change from OSW to ODW is a process that shows a continuous transition from deflagration to detonation conditions. OSW is generated at the tip of wedge when inflow enters the flow field, followed by a curved shock. A weak compression wave is formed between the OSW and curved shock to balance the pressure in the flow field. Therefore, a triple point is formed when inflow enters the flow field. A thin chemical reaction layer is formed on the

wedge surface, which shows KH instability near the wedge surface as well as slip line. However, the thickness of the reaction layer is limited by the reaction rate. With the passage of time, the reaction layer thickens due to the fast expansion rate of the reaction front, and the deflagration surface begins to form. The distance between the deflagration surface and the OSW decreases, and the intensity of deflagration gets higher, approaching CJ conditions. In this process, the new triple points are formed and propagate downstream along the wave front, which stabilizes the front of OSW and ODW behind. It indicates that the motion of the triple points can stabilize the uneven internal flow field until a stable ODW is formed.

A simple theoretical method to predict the triple point is proposed. The prediction model is analyzed and verified based on the numerical simulation results in this paper. The results show that, based on the assumptions in this paper, the error of the theoretical prediction model for the position of the triple point is relatively acceptable. However, more validation and accurate revisions for this model are expected in the future.

## DECLARATION OF COMPETING INTEREST

The authors declare that they have no known competing financial interests or personal relationships that could have appeared to influence the work reported in this paper.

## ACKNOWLEDGEMENTS

This work is supported by National Natural Science Foundation of China (Grant No. 51876182, 51406171 and 11972331), and Fundamental Research Funds for the Central Universities of China (Grant No. 20720180058).

## DATA AVAILABILITY

The data that support the findings of this study are available from the corresponding author upon reasonable request.

## References

[1] R.A. Gross, Oblique detonation waves, AIAA J. 1 (5) (1963) 1225-1227.

[2] D.T. Pratt, J.W. Humphrey, D.E. Glenn, Morphology of standing oblique detonation waves, J. Propuls. Power 7 (5) (1991) 837-845.

[3] J.M. Powers, Oblique detonations: theory and propulsion applications, in: J. Buckmaster, T.L. Jackson, A. Kumar (Eds), Combustion in High-Speed Flows, Kluwer Academic, Norwell, MA, 1994, PP. 345-371.

[4] C.I. Morris, M.R. Kamel, R.K. Hanson, Shock-induced combustion in high-speed wedge flows, Symp. (Int.) Combust. 27 (2) (1998) 2157-2164.

[5] D.S. Stewart, A.R. Kasimov, State of detonation stability theory and its application to propulsion, J. Propuls. Power 22 (6) (2006) 1230-1244.

[6] J. Urzay, Supersonic combustion in air-breathing propulsion systems for hypersonic flight, Annu. Rev. Fluid Mech. 50 (1) (2018) 593-627.

[7] J.M. Powers, K.A. Gonthier, Reaction zone structure for strong, weak overdriven, and weak underdriven oblique detonations, Phys. Fluids 4 (9) (1992) 2082-2089.

[8] J.M. Powers, D.S. Stewart, Approximate solutions for oblique detonations in the hypersonic limit, AIAA J. 30 (3) (1992) 726-736.

[9] G. Emanuel, D. Tuckness, Steady, oblique, detonation waves, Shock Waves 13 (6) (2004) 445-451.

[10] J. Verreault, A.J. Higgins, R.A. Stowe, Formation and structure of steady oblique and conical detonation waves, AIAA J. 50 (8) (2012) 1766-1772.

[11] D. Martínez-Ruiz, C. Huete, A.L. Sánchez, F.A. Williams, Theory of weakly exothermic oblique detonations, AIAA J. 58 (1) (2020) 236-242.

[12] D. Martinez-Ruiz, L. Scotzniovsky, A.L. Sanchez, F.A. Williams, Wedge-induced oblique detonations with small heat release, in: AIAA Scitech 2021 Forum, AIAA 2021-0287.

[13] C. Li, K. Kailasanath, E.S. Oran, Detonation structures behind oblique shocks, Phys. Fluids 6 (4) (1994) 1600-1611.

[14] V.V. Vlasenko, V.A. Sabel'Nikov, Numerical simulation of inviscid flows with hydrogen combustion behind shock waves and in detonation waves, Combust. Explos. Shock Waves 31 (3) (1995) 376-389.

379 [15] L.F.F. Da Silva, B. Deshaies, Stabilization of an oblique detonation wave by a wedge: a parametric numerical
380 study, Combust. Flame, 121 (1-2) (2000) 152-166.
381 [16] K. Ghorbanian, J.D. Sterling, Influence of formation processes on oblique detonation wave stabilization, J.
382 Propuls. Power 12 (3) (1996) 509-517.
383 [17] J.P. Sislian, R. Dudebout, J. Schumacher, M. Islam, T. Redford, Incomplete mixing and off-design effects on
384 shock-induced combustion ramjet performance, J. Propuls. Power 16 (1) (2000) 41-48.
385 [18] G. Fusina, J.P. Sislian, B. Parent, Formation and stability of near chapman-jouguet standing oblique detonation
386 waves, AIAA J. 43 (7) (2005) 1591-1604.
387 [19] Y. Zhang, J. Gong, T. Wang, Numerical study on initiation of oblique detonations in hydrogen–air mixtures with
388 various equivalence ratios, Aerosp. Sci. Technol. 49 (2016) 130-134.
389 [20] J.H.S. Lee, The Detonation Phenomenon, 2008.
390 [21] K. Iwata, S. Nakaya, M. Tsue, Numerical investigation of the effects of nonuniform premixing on shock-induced
391 combustion, AIAA J. 54 (5) (2016) 1682-1692.
392 [22] K. Iwata, S. Nakaya, M. Tsue, Wedge-stabilized oblique detonation in an inhomogeneous hydrogen–air mixture,
393 Proc. Combust. Inst. 36 (2) (2017) 2761-2769.
394 [23] Y. Fang, Z. Hu, H. Teng, Z. Jiang, H.D. Ng, Numerical study of inflow equivalence ratio inhomogeneity on
395 oblique detonation formation in hydrogen–air mixtures, Aerosp. Sci. Technol. 71 (2017) 256-263.
396 [24] C.L. Bachman, G.B. Goodwin, Ignition criteria and the effect of boundary layers on wedge-stabilized oblique
397 detonation waves, Combust. Flame, 223 (2021) 271-283.
398 [25] J.L. Ziegler, R. Deiterding, J.E. Shepherd, D.I. Pullin, An adaptive high-order hybrid scheme for compressive,
399 viscous flows with detailed chemistry, J. Comput. Phys. 230 (20) (2011) 7598-7630.
400 [26] R. Deiterding, A parallel adaptive method for simulating shock-induced combustion with detailed chemical
401 kinetics in complex domains, Comput. Struct. 87 (11-12) (2009) 769-783.

[27] M.J. Berger, J. Oliger, Adaptive mesh refinement for hyperbolic partial differential equations, J. Comput. Phys. 53 (3) (1984) 484-512.

[28] E.S. Oran, J.P. Boris, Numerical Simulation of Reactive Flow, 2nd edition, Cambridge University Press, 2001.

[29] M.P. Martín, E.M. Taylor, M. Wu, V.G. Weirs, A bandwidth-optimized WENO scheme for the effective direct numerical simulation of compressible turbulence, J. Comput. Phys. 220 (1) (2006) 270-289.

[30] S. Gottlieb, D.I. Ketcheson, C.-W. Shu, High order strong stability preserving time discretizations, J. Sci. Comput. 38 (3) (2008) 251-289.

[31] P. Kaps, P. Rentrop, Generalized Runge-Kutta methods of order four with stepsize control for stiff ordinary differential equations, Numer. Math. 33 (1) (1979) 55-68.

[32] C.K. Westbrook, Chemical kinetics of hydrocarbon oxidation in gaseous detonations, Combust. Flame, 46 (1982) 191-210.

[33] T. Wang, Y. Zhang, H. Teng, Z. Jiang, H.D. Ng, Numerical study of oblique detonation wave initiation in a stoichiometric hydrogen-air mixture, Phys. Fluids 27 (9) (2015) 096101.

[34] D.G. Goodwin, R.L. Speth, H.K. Moffat, B.W Weber, Cantera: An object-oriented software toolkit for chemical kinetics, thermodynamics, and transport processes, Version 2.4.0, (2018).

[35] C. Viguier, L.F.F. Da Silva, D. Desbordes, B. Deshaies, Onset of oblique detonation waves: Comparison between experimental and numerical results for hydrogen-air mixtures, Symp. (Int.) Combust. 26 (2) (1996) 3023-3031.

[36] Y. Huang, Z. Luan, Z. Li, H. Ji, Y. You, Study on the flow characteristics in the non-detonation reaction zones of wedge-induced oblique detonation transitions, Aerosp. Sci. Technol. 120 (2022) 107282.